

## Multi-Phase PWM Controller for Core-Voltage Regulation

The ISL6557A provides core-voltage regulation by driving up to four interleaved synchronous-rectified buck-converter channels in parallel. Intersil multi-phase controllers together with Intersil MOSFET drivers form the basis for the most reliable power-supply solutions available to power the latest industry-leading microprocessors. Multi-phase buck converter architecture uses interleaved timing to multiply ripple frequency and reduce input and output ripple currents. Lower ripple results in lower total component cost, reduced dissipation, and smaller implementation area. Pre-configured for 4-phase operation, the ISL6557A offers the flexibility of selectable 2- or 3-phase operation. Simply connect the unused PWM pins to VCC. The channel switching frequency is adjustable in the range of 50kHz to 1.5MHz giving the designer the ultimate flexibility in managing the balance between high-speed response and good thermal management.

New features on the ISL6557A include Dynamic-VID™ technology allowing seamless on-the-fly VID changes with no need for any additional external components. When the ISL6557A receives a new VID code, it incrementally steps the output voltage to the new level. Dynamic VID changes are fast and reliable with no output voltage overshoot or undershoot. The RGND and VSEN pins provide inputs for differential remote voltage sensing to improve regulation and protection accuracy. A threshold-sensitive enable pin (EN) can be used with an external resistor divider to optionally set the power-on voltage level. This allows optional start-up coordination with Intersil MOSFET drivers or any other devices powered from a separate supply.

Like other Intersil multiphase controllers, the ISL6557A uses cost and space-saving  $r_{DS(ON)}$  sensing for channel current balance, dynamic voltage positioning, and overcurrent protection. Channel current balancing is automatic and accurate with the integrated current-balance control system. Overcurrent protection can be tailored to any application with no need for additional parts. The IOUT pin carries a signal proportional to load current and can be optionally connected to FB for accurate load-line regulation.

An integrated DAC decodes the 5-bit logic signal present at VID4-VID0 and provides an accurate reference for precision voltage regulation. The high-bandwidth error amplifier, differential remote-sensing amplifier, and accurate voltage reference all work together to provide better than 0.8% total system accuracy, and to enable the fastest transient response available.

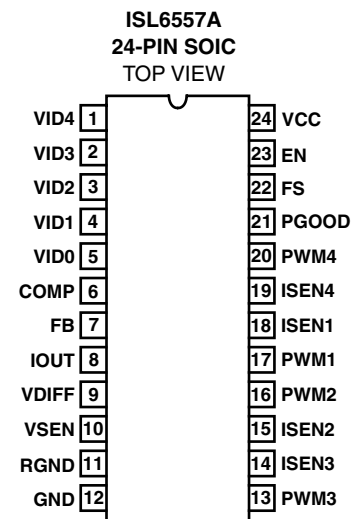
## Features

- Multi-Phase Power Conversion
- Active Channel Current Balancing
- Precision  $r_{DS(ON)}$  Current Sensing
  - Low Cost
  - Lossless
- Precision CORE Voltage Regulation
  - Differential Remote Voltage Sensing
  - $\pm 0.8\%$  System Accuracy
- Microprocessor Voltage Identification Input
  - Dynamic VID technology
  - 5-Bit VID Input
  - 1.100V to 1.850V in 25mV Steps
- Programmable Power-On Bias Level
- Programmable Droop Voltage
- Fast Transient Recovery Time
- Precision Enable Threshold
- Overcurrent Protection
- 2-, 3-, or 4-Phase Operation
- High Ripple Frequency. Channel Frequency Times Number Channels (100kHz to 6MHz)

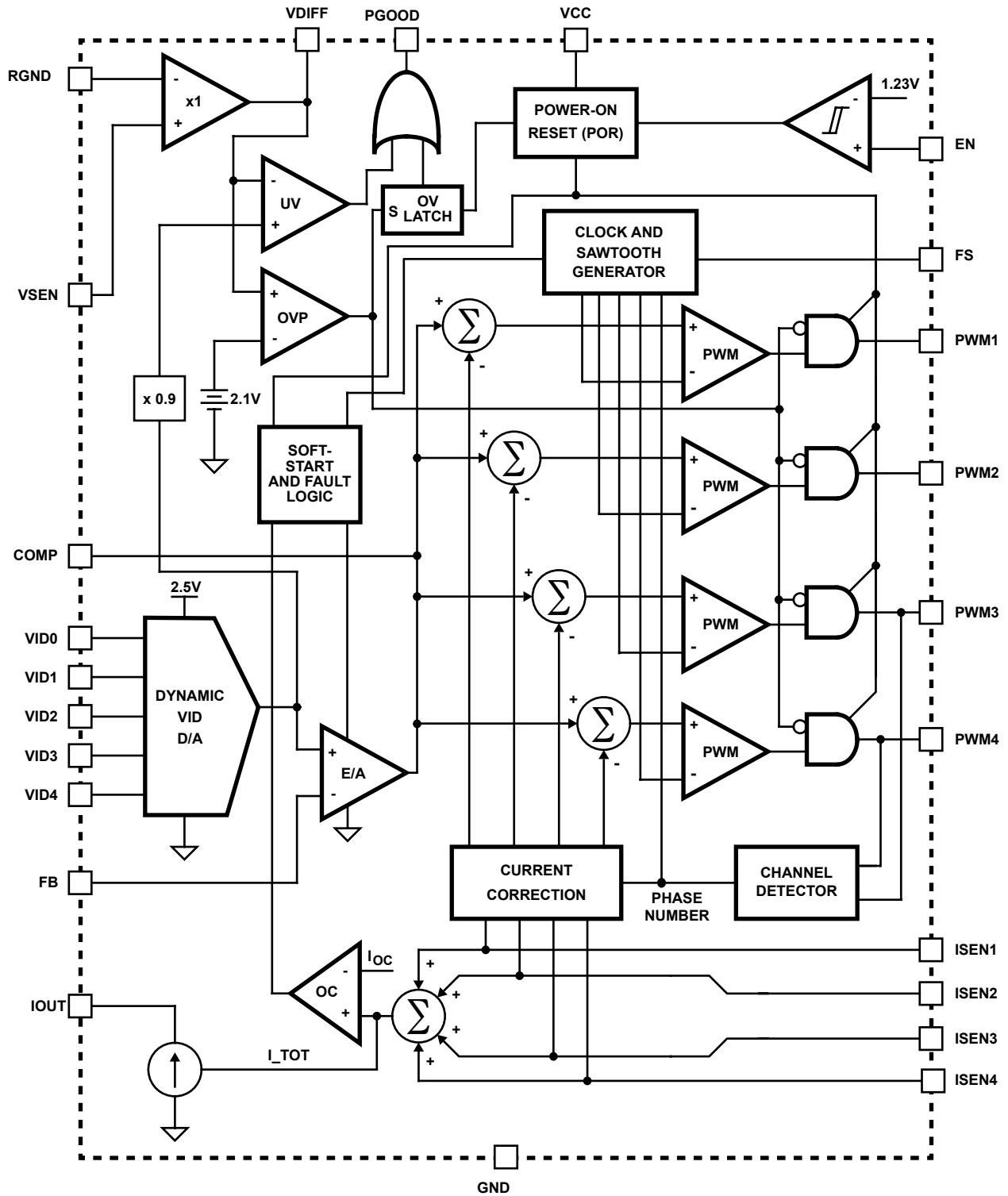
## Ordering Information

| PART NUMBER  | TEMP. (°C) | PACKAGE                  | PKG. NO. |
|--------------|------------|--------------------------|----------|
| ISL6557ACB   | 0 to 70    | 24-Ld SOIC               | M24.3    |
| ISL6557ACB-T |            | 20-Ld SOIC Tape and Reel |          |

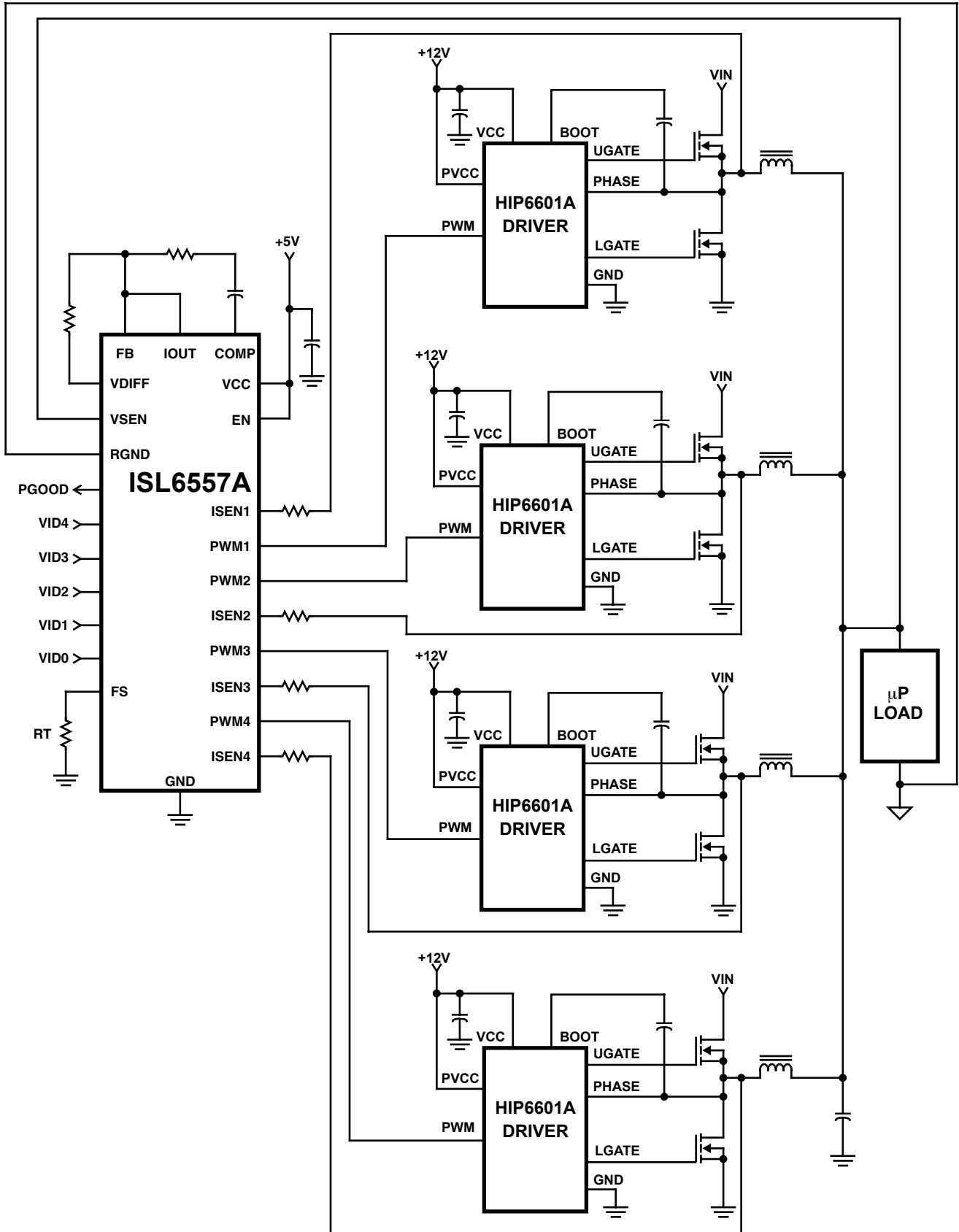
## Pinout



Block Diagram



Typical Application - 4-Phase Buck Converter



# ISL6557A

## Absolute Maximum Ratings

Supply Voltage, VCC . . . . . 7V  
 Input, Output, or I/O Voltage . . . . . GND -0.3V to V<sub>CC</sub> + 0.3V  
 ESD Classification . . . . . 1.5kV

## Recommended Operating Conditions

Supply Voltage . . . . . +5V ±5%  
 Ambient Temperature . . . . . 0°C to 70°C

## Thermal Information

Thermal Resistance (Typical, Note 1)  $\theta_{JA}$  (°C/W)  
 SOIC Package . . . . . 65  
 Maximum Junction Temperature . . . . . 150°C  
 Maximum Storage Temperature Range . . . . . -65°C to 150°C  
 Maximum Lead Temperature (Soldering 10s) . . . . . 300°C  
 (SOIC - Lead Tips Only)

*CAUTION: Stress above those listed in "Absolute Maximum Ratings" may cause permanent damage to the device. This is a stress only rating and operation of the device at these or any other conditions above those indicated in the operational section of this specification is not implied.*

### NOTE:

- $\theta_{JA}$  is measured with the component mounted on a high effective thermal conductivity test board in free air. (See Tech Brief TB379 for details.)

## Electrical Specifications

Operating Conditions: V<sub>CC</sub> = 5V, T<sub>A</sub> = 0°C to 70°C, Unless Otherwise Specified

| Parameter                     | Test Conditions                       | Min   | Typ   | Max   | Units      |
|-------------------------------|---------------------------------------|-------|-------|-------|------------|
| <b>INPUT SUPPLY POWER</b>     |                                       |       |       |       |            |
| Input Supply Current          | RT = 100k $\Omega$ , EN = 5V          |       | 10.5  | 15    | mA         |
|                               | RT = 100k $\Omega$ , EN = 0V          | 5     | 9.2   |       | mA         |
| Power-On Reset Threshold      | VCC Rising                            | 4.25  | 4.38  | 4.5   | V          |
|                               | VCC Falling                           | 3.75  | 3.86  | 4.0   | V          |
| Enable Threshold              | EN Rising                             | 1.206 | 1.230 | 1.254 | V          |
|                               | EN Falling                            | 1.106 | 1.15  | 1.194 | V          |
| Enable Hysteresis             |                                       | 60    |       | 100   | mV         |
| Enable Current                | EN = 3V                               |       |       | 50    | nA         |
| <b>SYSTEM ACCURACY</b>        |                                       |       |       |       |            |
| System Accuracy               | (Note 2)                              | -0.8  |       | 0.8   | %VID       |
| VID Pull Up                   |                                       | -40   | -20   | -10   | $\mu$ A    |
| VID Input Low Level           |                                       |       |       | 0.8   | V          |
| VID Input High Level (Note 3) |                                       | 2.0   |       |       | V          |
| <b>OSCILLATOR</b>             |                                       |       |       |       |            |
| Accuracy                      |                                       | -20   |       | 20    | %          |
| Frequency                     | RT = 110k $\Omega$ ( $\pm$ 1%)        |       | 250   |       | kHz        |
| Adjustment Range              |                                       | 80    |       | 1500  | kHz        |
| Sawtooth Amplitude            |                                       |       | 1.33  |       | V          |
| Duty-Cycle Range              |                                       | 0     |       | 75    | %          |
| <b>ERROR AMPLIFIER</b>        |                                       |       |       |       |            |
| Open-Loop Gain                | RL = 10k $\Omega$ to ground           |       | 72    |       | dB         |
| Open-Loop Bandwidth           | CL=100pF, RL = 10k $\Omega$ to ground |       | 18    |       | MHz        |
| Slew Rate                     | CL=100pF, RL = 10k $\Omega$ to ground |       | 5     |       | V/ $\mu$ s |
| Maximum Output Voltage        | RL = 10k $\Omega$ to ground           | 3.6   | 4.1   |       | V          |
| <b>REMOTE-SENSE AMPLIFIER</b> |                                       |       |       |       |            |
| Input Impedance               |                                       |       | 80    |       | k $\Omega$ |
| Slew Rate                     |                                       |       | 6     |       | V/ $\mu$ s |
| Bandwidth                     |                                       |       | 10    |       | MHz        |

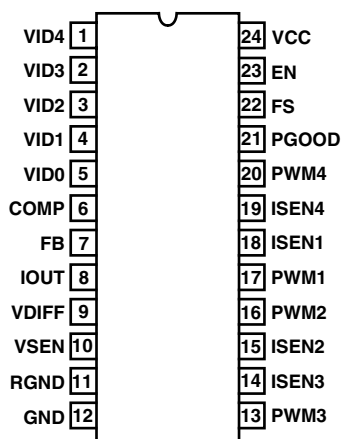
**Electrical Specifications** Operating Conditions:  $V_{CC} = 5V$ ,  $T_A = 0^{\circ}C$  to  $70^{\circ}C$ , Unless Otherwise Specified (Continued)

| Parameter                     | Test Conditions | Min  | Typ  | Max  | Units   |
|-------------------------------|-----------------|------|------|------|---------|
| <b>ISEN</b>                   |                 |      |      |      |         |
| Overcurrent Trip Level        |                 | -90  | -75  | -60  | $\mu A$ |
| <b>PROTECTION and MONITOR</b> |                 |      |      |      |         |
| Overvoltage Threshold         | VSEN Rising     | 2.04 | 2.09 | 2.13 | V       |
|                               | VSEN Falling    |      | VID  |      | V       |
| Undervoltage Threshold        | VSEN Rising     |      | 92   |      | %VID    |
|                               | VSEN Falling    |      | 90   |      | %VID    |
| PGOOD Low Voltage             | IPGOOD = 4mA    |      | 0.18 | 0.4  | mV      |

NOTES:

2. These parts are designed and adjusted for accuracy within the system tolerance given in the Electrical Specifications. The system tolerance accounts for offsets in the differential and error amplifiers; reference-voltage inaccuracies; temperature drift; and the full DAC adjustment range.
3. VID input levels above 2.9V may produce a reference-voltage offset inaccuracy.

**Functional Pin Descriptions**



**VID4, VID3, VID2, VID1, VID0 (Pins 1, 2, 3, 4, 5)**

These are the inputs to the internal DAC that provides the reference voltage for output regulation. Connect these pins to either open-drain or active-pull-up type outputs. Pulling these pins above 2.9V can cause a reference offset inaccuracy.

**FB (Pin 7) and COMP (Pin 6)**

The internal error amplifier's inverting input and output respectively. These pins are connected to an external R-C network to compensate the regulator.

**IOUT (Pin 8)**

The current out of this pin is proportional to output current and is used for load-line regulation and load sharing. The scale factor is set by the ratio of the ISEN resistors (connected to pins 14, 15, 18, and 19) to the lower MOSFET  $r_{DS(ON)}$ .

**VDIFF (Pin 9), VSEN (Pin 10), RGND (Pin 11)**

VSEN and RGND are the inputs to the differential remote-sense amplifier. VDIFF is the output and it serves as the

input to the external regulation circuitry and the internal protection circuitry. Connect VSEN and RGND to the sense pins of the remote load.

**GND (Pin 12)**

Return for VCC and signal ground for the IC.

**PWM3, PWM2, PWM1, PWM4 (Pins 13, 16, 17, 20)**

Pulse-width modulation outputs. These logic outputs tell the driver IC(s) when to turn the MOSFETs on and off.

**ISEN3, ISEN2, ISEN1, ISEN4 (PINS 14, 15, 18, 19)**

Current sense inputs. A resistor connected between these pins and the respective phase nodes has a current proportional to the current in the lower MOSFET during its conduction interval. The current is used as a reference for channel balancing, load sharing, protection, and load-line regulation.

**PGOOD (Pin 21)**

PGOOD is an open-drain logic output that changes to a logic low when the differential output voltage at VDIFF swings below 0.9V or above 2.1V.

**FS (Pin 22)**

This pin has two functions. A resistor placed from FS to ground sets the switching frequency. There is an inverse relationship between the value of the resistor and the switching frequency. This pin can also be used to disable the controller. To disable the controller, pull this pin below 1V.

**EN (Pin 23)**

This is the threshold-sensitive enable input for the controller. To enable the controller, pull this pin above 1.23V.

**VCC (Pin 24)**

Bias supply voltage for the controller. Connect this pin to a 5V power supply.

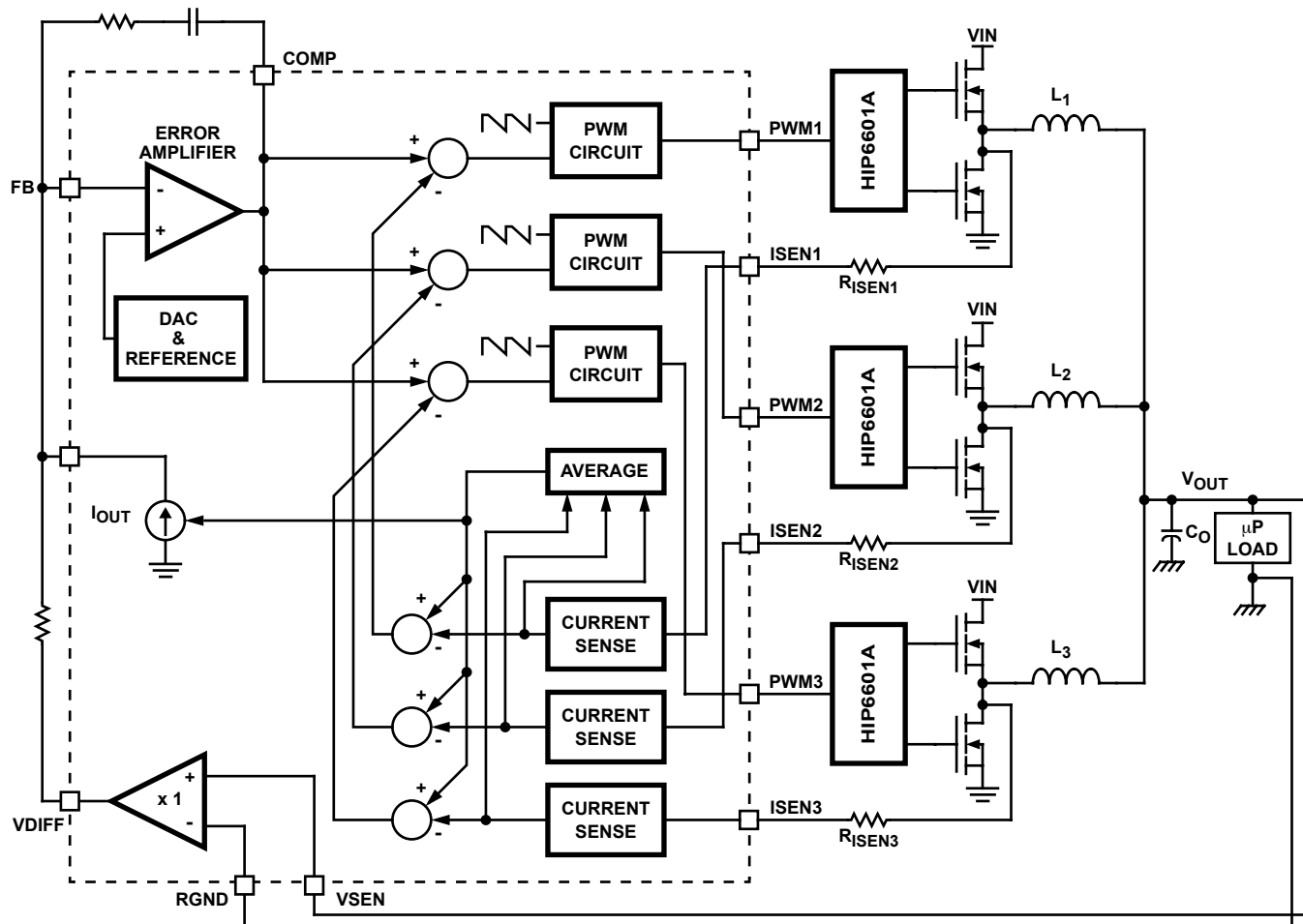


FIGURE 1. SIMPLIFIED BLOCK DIAGRAM OF THE ISL6557A IN A 3-PHASE CONVERTER

**Operation**

**Multi-Phase Power Conversion**

Multi-phase power conversion provides the most cost-effective power solution when load currents are no longer easily supported by single-phase converters. Although its greater complexity presents additional technical challenges, the multi-phase approach offers cost-saving advantages with improved response time, superior ripple cancellation, and excellent thermal distribution.

**INTERLEAVING**

The switching of each channel in a multi-phase converter is timed to be symmetrically out of phase with each of the other channels. In a 4-phase converter, each channel switches 1/4 cycle after the previous channel and 1/4 cycle before the following channel. As a result, the four-phase converter has a combined ripple frequency four times greater than the ripple frequency of any one phase. In addition, the peak-to-peak amplitude of the combined inductor currents is reduced in proportion to the number of phases (Equations 1 and 2). Increased ripple frequency and lower ripple amplitude mean

that the designer can use less per-channel inductance and lower total output capacitance for any performance specification.

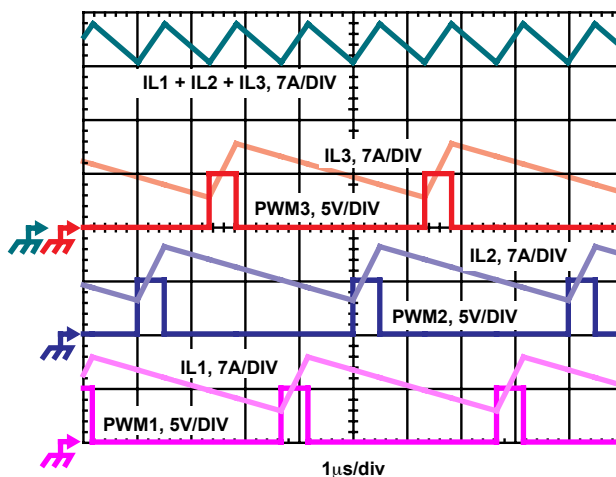


FIGURE 2. PWM AND INDUCTOR-CURRENT WAVEFORMS FOR 3-PHASE CONVERTER

Figure 2 (previous page) illustrates the multiplicative effect on output ripple frequency. The three channel currents (IL1, IL2, and IL3), combine to form the AC ripple current and the DC load current. The ripple component has three times the ripple frequency of each individual channel current. Each PWM pulse is terminated 1/3 of a cycle, or 1.33µs, after the PWM pulse of the previous phase. The peak-to-peak current waveforms for each phase is about 7A, and the dc components of the inductor currents combine to feed the load.

To understand the reduction of ripple current amplitude in the multi-phase circuit, examine the equation representing an individual channel's peak-to-peak inductor current.

$$I_{L,PP} = \frac{(V_{IN} - V_{OUT})V_{OUT}}{L f_S V_{IN}} \quad (\text{EQ. 1})$$

In Equation 1,  $V_{IN}$  and  $V_{OUT}$  are the input and output voltages respectively,  $L$  is the single-channel inductor value, and  $f_S$  is the switching frequency.

$$I_{PP} = \frac{(V_{IN} - N V_{OUT})V_{OUT}}{L f_S V_{IN}} \quad (\text{EQ. 2})$$

The output capacitors conduct the ripple component of the inductor current. In the case of multi-phase converters, the capacitor current is the sum of the ripple currents from each of the individual channels. Compare Equation 1 to the expression for the peak-to-peak current after the summation of  $N$  symmetrically phase-shifted inductor currents in Equation 2. Peak-to-peak ripple current decreases by an amount proportional to the number of channels. Output-voltage ripple is a function of capacitance, capacitor equivalent series resistance (ESR), and inductor ripple current. Reducing the inductor ripple current allows the designer to use fewer or less costly output capacitors.

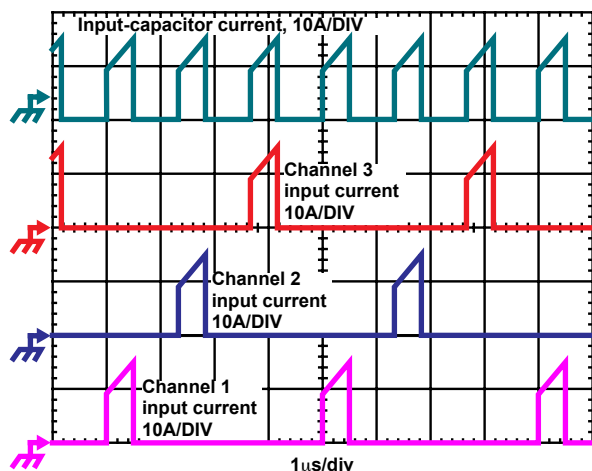


**FIGURE 3. CHANNEL INPUT CURRENTS AND INPUT-CAPACITOR RMS CURRENT FOR 3-PHASE CONVERTER**

Another benefit of interleaving is to reduce input ripple current. Input capacitance is determined in part by the

maximum input ripple current. Multi-phase topologies can improve overall system cost and size by lowering input ripple current and allowing the designer to reduce the cost of input capacitance. The example in Figure 3 illustrates input currents from a three-phase converter combining to reduce the total input ripple current.

The converter depicted in Figure 3 delivers 36A to a 1.5V load from a 12V input. The rms input capacitor current is 5.9A. Compare this to a single-phase converter also down 12V to 1.5V at 36A. The single-phase converter has 11.9A rms input capacitor current. The single-phase converter must use an input capacitor bank with twice the rms current capacity as the equivalent three-phase converter.

Figures 15, 16 and 17 the section entitled *Input Capacitor Selection* can be used to determine the input-capacitor rms current based on load current, duty cycle, and the number of channels. They are provided as aids in determining the optimal input capacitor solution. Figure 18 shows the single phase input-capacitor rms current for comparison.

## PWM OPERATION

The number of active channels selected determines the timing for each channel. By default, the timing mode for the ISL6557A is 4-phase. The designer can select 2-phase timing by connecting PWM3 to VCC or 3-phase timing by connecting PWM4 to VCC.

One switching cycle for the ISL6557A is defined as the time between PWM1 pulse termination signals (the internal signal that initiates a falling edge on PWM1). The cycle time is the inverse of the switching frequency selected by the resistor connected between the FS pin and ground (see *Switching Frequency*). Each cycle begins when a clock signal commands the channel-1 PWM output to go low. This signals the channel-1 MOSFET driver to turn off the channel-1 upper MOSFET and turn on the channel-1 synchronous MOSFET. If two-channel operation is selected, the PWM2 pulse terminates 1/2 of a cycle later. If three channels are selected the PWM2 pulse terminates 1/3 of a cycle after PWM1, and the PWM3 output will follow after another 1/3 of a cycle. When four channels are selected, the pulse-termination times are spaced in 1/4 cycle increments.

Once a channel's PWM pulse terminates, it remains low for a minimum of 1/4 cycle. This forced off time is required to assure an accurate current sample as described in *Current Sensing*. Following the 1/4-cycle forced off time, the controller enables the PWM output. Once enabled, the PWM output transitions high when the sawtooth signal crosses the adjusted error-amplifier output signal,  $V_{COMP}$  as illustrated in Figures 1 and 5. This is the signal for the MOSFET driver to turn off the synchronous MOSFET and turn on the upper MOSFET. The output will remain high until the clock signals the beginning of the next cycle by commanding the PWM pulse to terminate.

**CURRENT SENSING**

Intersil multi-phase controllers sense current by sampling the voltage across the lower MOSFET during its conduction interval. MOSFET  $r_{DS(ON)}$  sensing is a no-added-cost method to sense current for load-line regulation, channel-current balance, module current sharing, and overcurrent protection. If desired, an independent current-sense resistor in series with the lower-MOSFET source can serve as a sense element in place of the MOSFET  $r_{DS(ON)}$ .

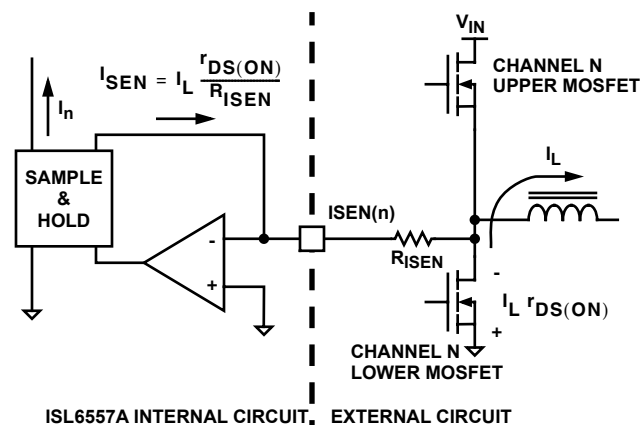


**FIGURE 4. INTERNAL AND EXTERNAL CURRENT-SENSING CIRCUITRY**

The ISEN input for each channel uses a ground-referenced amplifier to reproduce a signal proportional to the channel current (Figure 4). After sufficient settling time, the sensed current is sampled, and the sample is used for current balance, load-line regulation and overcurrent protection. The ISL6557A samples channel current once each cycle. Figure 4 shows how the sampled current,  $I_n$ , is created from the channel current  $I_L$ . The circuitry in Figure 4 represents the current measurement and sampling circuitry for channel n in an N-channel converter. This circuitry is repeated for each channel in the converter but may not be active in channels 3 and 4 depending on the particular implementation (see *PWM Operation*).

**CHANNEL-CURRENT BALANCE**

Another benefit of multi-phase operation is the thermal advantage gained by distributing the dissipated heat over multiple devices and greater area. By doing this, the designer avoids the complexity of driving multiple parallel MOSFETs and the expense of using expensive heat sinks and exotic magnetic materials.

In order to fully realize the thermal advantage, it is important that each channel in a multi-phase converter be controlled to deliver about the same current at any load level. Intersil multi-phase controllers guarantee current balance by comparing each channel's current to the average current delivered by all channels and making an appropriate adjustment to each channel's pulse width based on the error. Intersil's patented current-balance method is illustrated in Figure 5 where the average of the 2, 3, or 4 sampled

channel currents combines with the channel 1 sample,  $I_1$ , to create an error signal  $I_{ER}$ . The filtered error signal modifies the pulse width commanded by  $V_{COMP}$  to correct any unbalance and force  $I_{ER}$  toward zero.

In some circumstances, it may be necessary to deliberately design some channel-current unbalance into the system. In a highly compact design, one or two channels may be able to cool more effectively than the other(s) due to nearby air flow or heat sinking components. The other channel(s) may have more difficulty cooling with comparatively less air flow and heat sinking. The hotter channels may also be located close to other heat-generating components tending to drive their temperature even higher. In these cases, a proper selection of the current sense resistors ( $R_{ISEN}$  in Figure 4) introduces channel current unbalance into the system. Increasing the value of  $R_{ISEN}$  in the cooler channels and decreasing it in the hotter channels moves all channels into thermal balance at the expense of current balance.

**OVERCURRENT PROTECTION**

The average current,  $I_{AVG}$  in Figure 5, is continually compared with a constant  $75\mu A$  reference current. If the average current at any time exceeds the reference current, the comparator triggers the converter to shut down. All PWM signals are placed in a high-impedance state which signals the drivers to turn off both upper and lower MOSFETs. The system remains in this state while the controller counts 2048 phase-clock cycles.

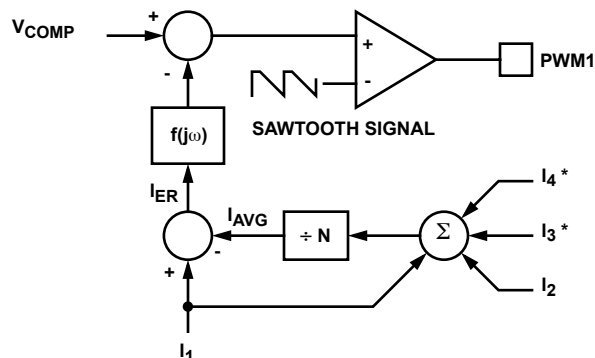


**FIGURE 5. CHANNEL-1 PWM FUNCTION AND CURRENT-BALANCE ADJUSTMENT**

NOTE: \*Channels 3 and 4 are optional.

This is followed by a soft-start attempt (see *Soft-Start*). If the soft-start attempt is successful, operation will continue as normal. Should the soft-start attempt fail, the ISL6557A repeats the 2048-cycle wait period and follows with another soft-start attempt. This hiccup mode of operation continues



indefinitely as shown in Figure 6 as long as the controller is enabled or until the overcurrent condition resolves.

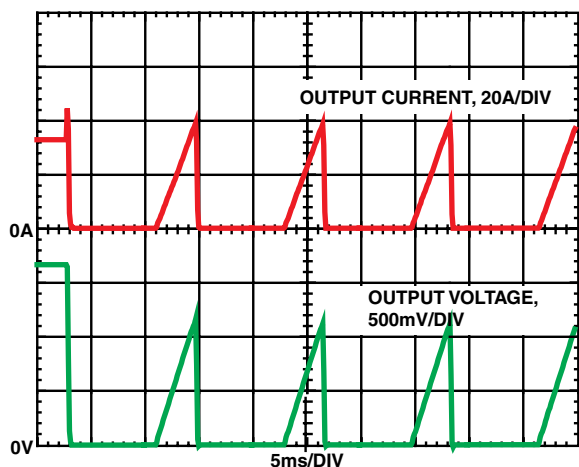


FIGURE 6. OVERCURRENT BEHAVIOR IN HICCUP MODE

### VOLTAGE REGULATION

The ISL6557A uses a digital to analog converter (DAC) to generate a reference voltage based on the logic signals at pins VID4 to VID0. The DAC decodes the a 5-bit logic signal (VID) into one of the discrete voltages shown in Table 1. Each VID input offers a 20 $\mu$ A pull up to 2.5V for use with open-drain outputs. External pull-up resistors or active-high output stages can augment the pull-up current sources, but a slight accuracy error can occur if they are pulled above 2.9V.

The DAC-selected reference voltage is connected to the non-inverting input of the error amplifier, and the output of the differential remote-sense amplifier usually gets connected to the error amplifier as shown in Figure 7. The remote-sense amplifier eliminates voltage differences between local and remote ground to provide a more accurate means of sensing output voltage.

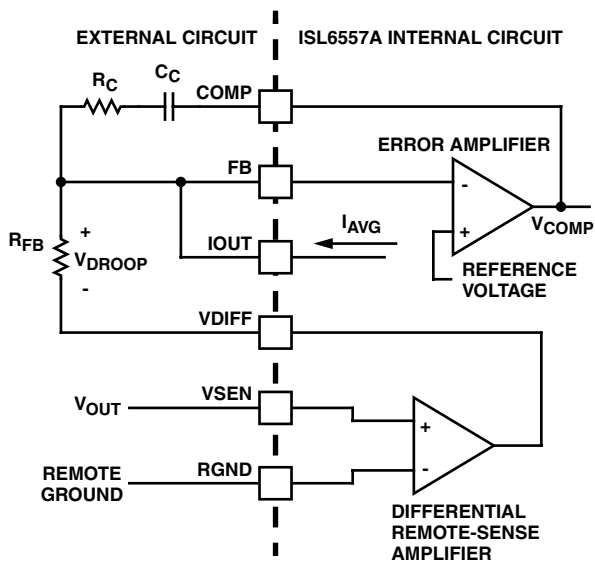


FIGURE 7. OUTPUT-VOLTAGE AND LOAD-LINE REGULATION

The integrating compensation network shown in Figure 7 assures that the steady-state error in the output voltage is limited to the error in the reference voltage (output of the DAC) plus offset errors in the remote-sense and error amplifiers. Intersil specifies the guaranteed tolerance of the ISL6557A and all Intersil controllers to include all variations in the amplifiers and reference so that the output voltage remains within the specified system tolerance.

TABLE 1. VOLTAGE IDENTIFICATION CODES

| VID4 | VID3 | VID2 | VID1 | VID0 | VDAC  |
|------|------|------|------|------|-------|
| 1    | 1    | 1    | 1    | 1    | Off   |
| 1    | 1    | 1    | 1    | 0    | 0.800 |
| 1    | 1    | 1    | 0    | 1    | 0.825 |
| 1    | 1    | 1    | 0    | 0    | 0.850 |
| 1    | 1    | 0    | 1    | 1    | 0.875 |
| 1    | 1    | 0    | 1    | 0    | 0.900 |
| 1    | 1    | 0    | 0    | 1    | 0.925 |
| 1    | 1    | 0    | 0    | 0    | 0.950 |
| 1    | 0    | 1    | 1    | 1    | 0.975 |
| 1    | 0    | 1    | 1    | 0    | 1.000 |
| 1    | 0    | 1    | 0    | 1    | 1.025 |
| 1    | 0    | 1    | 0    | 0    | 1.050 |
| 1    | 0    | 0    | 1    | 1    | 1.075 |
| 1    | 0    | 0    | 1    | 0    | 1.100 |
| 1    | 0    | 0    | 0    | 1    | 1.125 |
| 1    | 0    | 0    | 0    | 0    | 1.150 |
| 0    | 1    | 1    | 1    | 1    | 1.175 |
| 0    | 1    | 1    | 1    | 0    | 1.200 |
| 0    | 1    | 1    | 0    | 1    | 1.225 |
| 0    | 1    | 1    | 0    | 0    | 1.250 |
| 0    | 1    | 0    | 1    | 1    | 1.275 |
| 0    | 1    | 0    | 1    | 0    | 1.300 |
| 0    | 1    | 0    | 0    | 1    | 1.325 |
| 0    | 1    | 0    | 0    | 0    | 1.350 |
| 0    | 0    | 1    | 1    | 1    | 1.375 |
| 0    | 0    | 1    | 1    | 0    | 1.400 |
| 0    | 0    | 1    | 0    | 1    | 1.425 |
| 0    | 0    | 1    | 0    | 0    | 1.450 |
| 0    | 0    | 0    | 1    | 1    | 1.475 |
| 0    | 0    | 0    | 1    | 0    | 1.500 |
| 0    | 0    | 0    | 0    | 1    | 1.525 |
| 0    | 0    | 0    | 0    | 0    | 1.550 |

### OVERVOLTAGE PROTECTION

The ISL6557A detects output voltages above 2.1V and immediately commands all PWM outputs low. This directs the Intersil drivers turn on the lower MOSFETs and protect the load by preventing any further increase in output voltage. Once the output voltage falls to the level set by the VID code, the PWM outputs enter high-impedance mode. The Intersil drivers respond by turning off both upper and lower MOSFETs. If the overvoltage condition reoccurs, the ISL6557A will again command the lower MOSFETs to turn on. The ISL6557A will continue to protect the load in this fashion as long as the overvoltage repeats.

After detecting an overvoltage condition, the ISL6557A ceases normal PWM operation until it is reset by power cycle in which VCC is removed below the POR falling threshold and restored above the POR rising threshold as described in *Enable and Disable* and *Electrical Specifications*.

### LOAD-LINE REGULATION

In applications with high transient current slew rates, the lowest-cost solution for maintaining regulation often requires some kind of controlled output impedance. Pin 8 of the ISL6557A carries a current proportional to the average current of all active channels. The current is equivalent to  $I_{AVG}$  in Figures 5 and 7. Connecting FB and IOOUT together forces  $I_{AVG}$  into the summing node of the error amplifier and produces a voltage drop across the feedback resistor,  $R_{FB}$ , proportional to the output current. In Figure 7, the steady-state value of  $V_{DROOP}$  is simply

$$V_{DROOP} = I_{AVG} R_{FB} \quad (EQ. 3)$$

In the case that each channel uses the same value for  $R_{ISEN}$  to sense channel current, and this is almost always true, a more complete expression for  $V_{DROOP}$  can be determined from the expression for  $I_{AVG}$  as it is derived from Figures 4 and 5.

$$I_{AVG} = \frac{I_{OUT}}{N} \frac{r_{DS(ON)}}{R_{ISEN}} \quad (EQ. 4)$$

$$V_{DROOP} = \frac{I_{OUT}}{N} \frac{r_{DS(ON)}}{R_{ISEN}} R_{FB}$$

### ENABLE AND DISABLE

The internal power-on reset circuit (POR) prevents the ISL6557A from starting before the bias voltage at VCC reaches the POR-rising threshold as defined in *Electrical Specifications*. The POR level is high enough to guarantee that all parts of the ISL6557A can perform their functions properly. Built-in hysteresis assures that once enabled, the ISL6557A will not turn off unless the bias voltage falls to approximately 0.5V below the POR-rising level. When VCC

is below the POR-rising threshold, the PWM outputs are held in a high-impedance state to assure the drivers remain off.

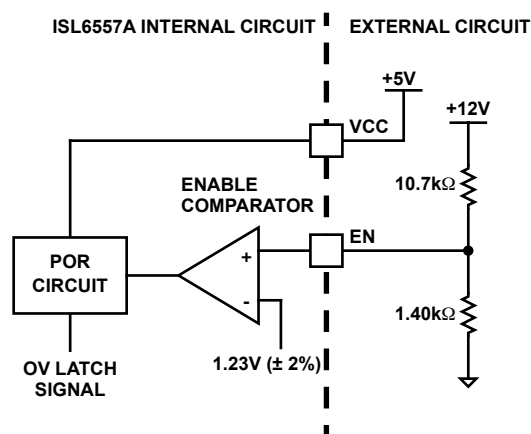


FIGURE 8. START-UP CONDITION USING THRESHOLD-SENSITIVE ENABLE (EN) FUNCTION

After power on, the ISL6557A remains in shut-down mode until the voltage at the enable input (EN) rises above 1.23V ( $\pm 2\%$ ). This optional feature prevents the ISL6557A from operating until the connected voltage rail is available and above some selectable threshold. For example, the HIP660X family of MOSFET driver ICs require 12V bias, and in certain circumstances, it can be important to assure that the drivers reach their POR level before the ISL6557A becomes enabled. The schematic in Figure 8 demonstrates coordination of the ISL6557A with HIP660X family of MOSFET driver ICs. The enable comparator has about 70mV of hysteresis to prevent bounce. To defeat the threshold-sensitive enable, connect EN to VCC.

The 11111 VID code is reserved as a signal to the controller that no load is present. The controller will enter shut-down mode after receiving this code and will start up upon receiving any other code.

To enable the controller, VCC must be greater than the POR threshold; the voltage on EN must be greater than 1.23V; and VID cannot be equal to 11111. Once these conditions are true, the controller immediately initiates a soft start sequence.

### SOFT-START

The soft-start time,  $t_{SS}$ , is determined by an 11-bit counter that increments with every pulse of the phase clock. For example, a converter switching at 250kHz has a soft-start time of

$$T_{SS} = \frac{2048}{f_{SW}} = 8.2ms \quad (EQ. 5)$$

During the soft-start interval, the soft-start voltage,  $V_{RAMP}$ , increases linearly from zero to 140% of the programmed DAC voltage. At the same time a current source,  $I_{RAMP}$ , is decreasing from 160 $\mu$ A down to zero. These signals are connected as shown in Figure 9 ( $I_{OUT}$  may or may not be connected to FB depending on the particular application).

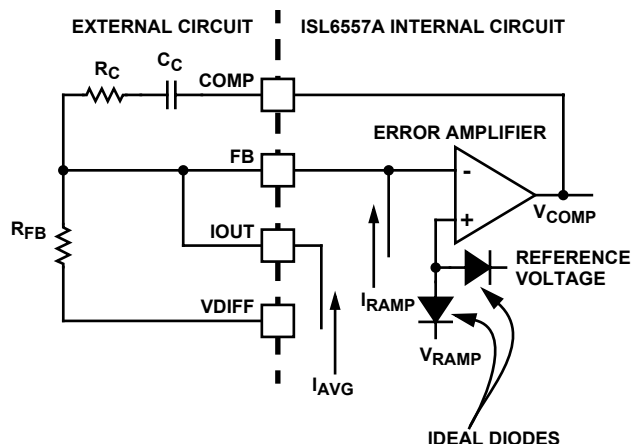


**FIGURE 9. RAMP CURRENT AND VOLTAGE FOR REGULATING SOFT-START SLOPE AND DURATION**

The ideal diodes in Figure 9 assure that the controller tries to regulate its output to the lower of either the reference voltage or  $V_{RAMP}$ . Since  $I_{RAMP}$  creates an initial offset across  $R_{FB}$  of  $R_{FB}$  times 160 $\mu$ A, the first PWM pulses will not be seen until  $V_{RAMP}$  is greater than the  $R_{FB}I_{RAMP}$  offset. This produces a delay after the ISL6557A enables before the output voltage starts moving. For example, if VID = 1.5V,  $R_{FB}$  = 1k $\Omega$  and  $T_{SS}$  = 8.3ms, the delay time can be expressed using Equation 6.

$$t_{DELAY} = \frac{T_{SS}}{1 + \frac{1.4(VID)}{R_{FB}160 \times 10^{-6}}} = 580\mu s \quad (EQ. 6)$$

From this point, the soft start ramps linearly until  $V_{RAMP}$  reaches VID. For the system described above, this first linear ramp will continue for approximately

$$t_{RAMP1} = \frac{T_{SS}}{1.4} - t_{DELAY} = 5.27ms \quad (EQ. 7)$$

The final portion of the soft-start sequence is the time remaining after  $V_{RAMP}$  reaches VID and before  $I_{RAMP}$  gets to zero. This is also characterized by a slight linear ramp in the output voltage which, for the current example, exists for a time

$$t_{RAMP2} = T_{SS} - t_{RAMP1} - t_{DELAY} = 2.34ms \quad (EQ. 8)$$

This behavior is seen in the example in Figure 10 of a converter switching at 500kHz. For this converter,  $R_{FB}$  is set to 2.67k $\Omega$

leading to  $T_{SS}$  = 4.0ms,  $t_{DELAY}$  = 700ns,  $t_{RAMP1}$  = 2.23ms, and  $t_{RAMP2}$  = 1.17ms.

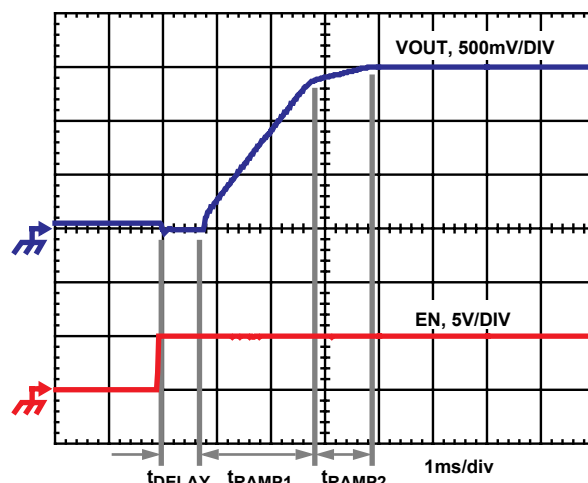


**FIGURE 10. SOFT-START WAVEFORMS FOR ISL6557A BASED MULTI-PHASE BUCK CONVERTER**

NOTE: Switching frequency 500kHz and  $R_{FB}$  = 2.67k $\Omega$

### DYNAMIC VID

The ISL6557A is capable of executing on-the-fly output-voltage changes. At the beginning of the phase-1 switching cycle (defined in the section entitled *PWM Operation*), the ISL6557A checks for a change in the VID code. The VID code is the bit pattern present at pins VID4-VID0 as outlined in *Voltage Regulation*. If the new code remains stable for another full cycle, the ISL6557A begins incrementing the reference by making 25mV change every two switching cycles until the it reaches the new VID code.

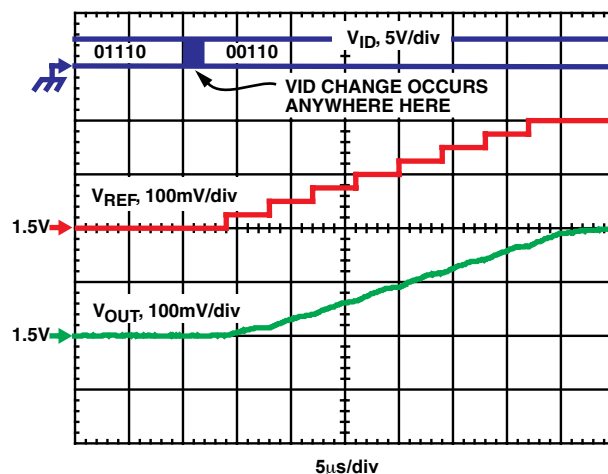


**FIGURE 11. DYNAMIC-VID WAVEFORMS FOR 500KHZ ISL6557A BASED MULTI-PHASE BUCK CONVERTER**

Since the ISL6557A recognizes VID-code changes only at the beginnings of switching cycles, up to one full cycle may pass before a VID change registers. This is followed by a one-cycle wait before the output voltage begins to change. Thus, the total time required for a VID change,  $t_{DV}$ , is

dependent on the switching frequency ( $f_S$ ), the size of the change ( $\Delta V_{ID}$ ), and the time before the next switching cycle begins. The one-cycle uncertainty in Equation 9 is due to the possibility that the VID code change may occur up to one full cycle before being recognized. The time required for a converter running with  $f_S = 500\text{kHz}$  to make a 1.5V to 1.7V reference-voltage change is between 30 $\mu\text{s}$  and 32 $\mu\text{s}$  as calculated using Equation 9. This example is also illustrated in Figure 11.

$$\frac{1}{f_S} \left( \frac{2\Delta V_{ID}}{0.025} - 1 \right) < t_{DV} \leq \frac{1}{f_S} \left( \frac{2\Delta V_{ID}}{0.025} \right) \quad (\text{EQ. 9})$$

## General Design Guide

This design guide is intended to provide a high-level explanation of the steps necessary to create a multi-phase power converter. It is assumed that the reader is familiar with many of the basic skills and techniques referenced below. In addition to this guide, Intersil provides complete reference designs that include schematics, bills of materials, and example board layouts for all common microprocessor applications.

### Power Stages

The first step in designing a multi-phase converter is to determine the number of phases. This determination depends heavily on the cost analysis which in turn depends on system constraints that differ from one design to the next. Principally, the designer will be concerned with whether components can be mounted on both sides of the circuit board; whether through-hole components are permitted on either side; and the total board space available for power-supply circuitry. Generally speaking, the most economical solutions will be for each phase to handle between 15 and 20A. All-surface-mount designs will tend toward the lower end of this current range and, if through-hole MOSFETs can be used, higher per-phase currents are possible. In cases where board space is the limiting constraint, current can be pushed as high as 30A per phase, but these designs require heat sinks and forced air to cool the MOSFETs.

### MOSFETs

The choice of MOSFETs depends on the current each MOSFET will be required to conduct; the switching frequency; the capability of the MOSFETs to dissipate heat; and the availability and nature of heat sinking and air flow.

### LOWER MOSFET POWER CALCULATION

The calculation for heat dissipated in the lower MOSFET is simple, since virtually all of the heat loss in the lower MOSFET is due to current conducted through the channel resistance ( $r_{DS(ON)}$ ). In Equation 10,  $I_M$  is the maximum continuous output current;  $I_{L,PP}$  is the peak-to-peak inductor current (see Equation 1);  $d$  is the duty cycle ( $V_{OUT}/V_{IN}$ ); and  $L$  is the per-channel inductance.

$$P_{LOW,1} = r_{DS(ON)} \left[ \left( \frac{I_M}{N} \right)^2 (1-d) + \frac{I_{L,PP}^2 (1-d)}{12} \right] \quad (\text{EQ. 10})$$

An additional term can be added to the lower-MOSFET loss equation to account for additional loss accrued during the dead time when inductor current is flowing through the lower-MOSFET body diode. This term is dependent on the diode forward voltage at  $I_M$ ,  $V_{D(ON)}$ ; the switching frequency,  $f_S$ ; and the length of dead times,  $t_{d1}$  and  $t_{d2}$ , at the beginning and the end of the lower-MOSFET conduction interval respectively.

$$P_{LOW,2} = V_{D(ON)} f_S \left[ \left( \frac{I_M}{N} + \frac{I_{PP}}{2} \right) t_{d1} + \left( \frac{I_M}{N} - \frac{I_{PP}}{2} \right) t_{d2} \right] \quad (\text{EQ. 11})$$

Thus the total power dissipated in each lower MOSFET is approximated by the summation of  $P_L$  and  $P_D$ .

### UPPER MOSFET POWER CALCULATION

In addition to  $r_{DS(ON)}$  losses, a large portion of the upper-MOSFET losses are due to currents conducted across the input voltage ( $V_{IN}$ ) during switching. Since a substantially higher portion of the upper-MOSFET losses are dependant on switching frequency, the power calculation is somewhat more complex. Upper MOSFET losses can be divided into separate components involving the upper-MOSFET switching times; the lower-MOSFET body-diode reverse-recovery charge,  $Q_{rr}$ ; and the upper MOSFET  $r_{DS(ON)}$  conduction loss.

When the upper MOSFET turns off, the lower MOSFET does not conduct any portion of the inductor current until the voltage at the phase node falls below ground. Once the lower MOSFET begins conducting, the current in the upper MOSFET falls to zero as the current in the lower MOSFET ramps up to assume the full inductor current. In Equation 12, the required time for this commutation is  $t_1$  and the associated power loss is  $P_{UP,1}$ .

$$P_{UP,1} \approx V_{IN} \left( \frac{I_M}{N} + \frac{I_{L,PP}}{2} \right) \left( \frac{t_1}{2} \right) f_S \quad (\text{EQ. 12})$$

Similarly, the upper MOSFET begins conducting as soon as it begins turning on. In Equation 13, this transition occurs over a time  $t_2$ , and the approximate the power loss is  $P_{UP,2}$ .

$$P_{UP,2} \approx V_{IN} \left( \frac{I_M}{N} - \frac{I_{L,PP}}{2} \right) \left( \frac{t_2}{2} \right) f_S \quad (\text{EQ. 13})$$

A third component involves the lower MOSFET's reverse-recovery charge,  $Q_{rr}$ . Since the inductor current has fully commutated to the upper MOSFET before the lower-MOSFET's body diode can recover all of  $Q_{rr}$ , it is conducted through the upper MOSFET across  $V_{IN}$ . The power dissipated as a result is  $P_{UP,3}$  and is simply

$$P_{UP,3} = V_{IN} Q_{rr} f_S \quad (\text{EQ. 14})$$

Finally, the resistive part of the upper MOSFET's is given in Equation 15 as  $P_{UP,4}$ .

$$P_{UP,4} = r_{DS(ON)} \left[ \left( \frac{I_M}{N} \right)^2 d + \frac{I_{PP}^2}{12} \right] \quad (\text{EQ. 15})$$

In this case, of course,  $r_{DS(ON)}$  is the on resistance of the upper MOSFET.

The total power dissipated by the upper MOSFET at full load can now be approximated as the summation of the results from Equations 12, 13, 14 and 15. Since the power equations depend on MOSFET parameters, choosing the correct MOSFETs can be an iterative process that involves repetitively solving the loss equations for different MOSFETs and different switching frequencies until converging upon the best solution.

### Current Sensing

Pins 18, 15, 14 and 19 are the ISEN pins denoted ISEN1, ISEN2, ISEN3 and ISEN4 respectively. The resistors connected between these pins and the phase nodes determine the gains in the load-line regulation loop and the channel-current balance loop. Select the values for these resistors based on the room temperature  $r_{DS(ON)}$  of the lower MOSFETs; the full-load operating current,  $I_{FL}$ ; and the number of phases,  $N$  according to Equation 16 (see also Figure 4).

$$R_{ISEN} = \frac{r_{DS(ON)} I_{FL}}{50 \times 10^{-6} N} \quad (\text{EQ. 16})$$

In certain circumstances, it may be necessary to adjust the value of one or more of the ISEN resistors. This can arise when the components of one or more channels are inhibited from dissipating their heat so that the affected channels run hotter than desired (see the section entitled *Channel-Current Balance*). In these cases, choose new, smaller values of  $R_{ISEN}$  for the affected phases. Choose  $R_{ISEN,2}$  in proportion to the desired decrease in temperature rise in order to cause proportionally less current to flow in the hotter phase.

$$R_{ISEN,2} = R_{ISEN} \frac{\Delta T_2}{\Delta T_1} \quad (\text{EQ. 17})$$

In Equation 17, make sure that  $\Delta T_2$  is the desired temperature rise above the ambient temperature, and  $\Delta T_1$  is the measured temperature rise above the ambient temperature. While a single adjustment according to Equation 17 is usually sufficient, it may occasionally be necessary to adjust  $R_{ISEN}$  two or more times to achieve perfect thermal balance between all channels.

### Load-Line Regulation Resistor

The load-line regulation resistor is labeled  $R_{FB}$  in Figure 7. Its value depends on the desired full-load droop voltage ( $V_{DROOP}$  in Figure 7). If Equation 16 is used to select each

ISEN resistor, the load-line regulation resistor is as shown in Equation 18.

$$R_{FB} = \frac{V_{DROOP}}{50 \times 10^{-6}} \quad (\text{EQ. 18})$$

If one or more of the ISEN resistors was adjusted for thermal balance as in Equation 17, the load-line regulation resistor should be selected according to Equation 19 where  $I_{FL}$  is the full-load operating current and  $R_{ISEN(n)}$  is the ISEN resistor connected to the  $n^{\text{th}}$  ISEN pin.

$$R_{FB} = \frac{V_{DROOP}}{I_{FL} r_{DS(ON)}} \sum_n R_{ISEN(n)} \quad (\text{EQ. 19})$$

### Compensation

The two opposing goals of compensating the voltage regulator are stability and speed. Depending on whether the regulator employs the optional load-line regulation as described in *Load-Line Regulation*, there are two distinct methods for achieving these goals.

### COMPENSATING A LOAD-LINE REGULATED CONVERTER

The load-line regulated converter behaves in a similar manner to a peak-current mode controller because the two poles at the output-filter L-C resonant frequency split with the introduction of current information into the control loop. The final location of these poles is determined by the system function, the gain of the current signal, and the value of the compensation components,  $R_C$  and  $C_C$ .

Since the system poles and zero are effected by the values of the components that are meant to compensate them, the solution to the system equation becomes fairly complicated. Fortunately there is a simple approximation that comes very close to an optimal solution. Treating the system as though it were a voltage-mode regulator by compensating the L-C poles and the ESR zero of the voltage-mode approximation yields a solution that is always stable with very close to ideal transient performance.

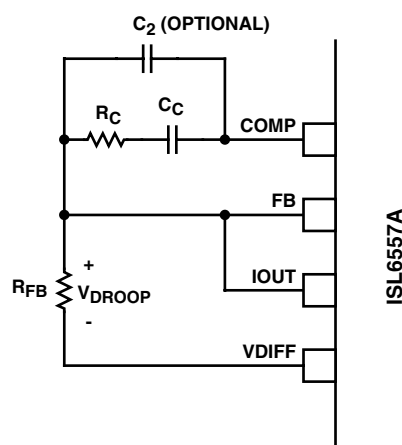


FIGURE 12. COMPENSATION CONFIGURATION FOR LOAD-LINE REGULATED ISL6557A CIRCUIT

The feedback resistor,  $R_{FB}$ , has already been chosen as outlined in *Load-Line Regulation Resistor*. Select a target bandwidth for the compensated system,  $f_0$ . The target bandwidth must be large enough to assure adequate transient performance, but smaller than 1/3 of the per-channel switching frequency. The values of the compensation components depend on the relationships of  $f_0$  to the L-C pole frequency and the ESR zero frequency. For each of the three cases defined below, there is a separate set of equations for the compensation components.

Case 1:  $\frac{1}{2\pi\sqrt{LC}} > f_0$

$$R_C = R_{FB} \frac{2\pi f_0 V_{PP} \sqrt{LC}}{0.75 V_{IN}}$$

$$C_C = \frac{0.75 V_{IN}}{2\pi V_{PP} R_{FB} f_0}$$

Case 2:  $\frac{1}{2\pi\sqrt{LC}} \leq f_0 < \frac{1}{2\pi C(ESR)}$

$$R_C = R_{FB} \frac{V_{PP}(2\pi)^2 f_0^2 LC}{0.75 V_{IN}} \quad (EQ. 20)$$

$$C_C = \frac{0.75 V_{IN}}{(2\pi)^2 f_0^2 V_{PP} R_{FB} \sqrt{LC}}$$

Case 3:  $f_0 > \frac{1}{2\pi C(ESR)}$

$$R_C = R_{FB} \frac{2\pi f_0 V_{PP} L}{0.75 V_{IN} (ESR)}$$

$$C_C = \frac{0.75 V_{IN} (ESR) \sqrt{C}}{2\pi V_{PP} R_{FB} f_0 \sqrt{L}}$$

In Equations 20, L is the per-channel filter inductance divided by the number of active channels; C is the sum total of all output capacitors; ESR is the equivalent-series resistance of the bulk output-filter capacitance; and  $V_{PP}$  is the peak-to-peak sawtooth signal amplitude as described in Figure 5 and *Electrical Specifications*.

Once selected, the compensation values in Equations 20 assure a stable converter with reasonable transient performance. In most cases, transient performance can be improved by making adjustments to  $R_C$ . Slowly increase the value of  $R_C$  while observing the transient performance on an oscilloscope until no further improvement is noted. Normally,  $C_C$  will not need adjustment. Keep the value of  $C_C$  from Equations 20 unless some performance issue is noted.

The optional capacitor  $C_2$ , is sometimes needed to bypass noise away from the PWM comparator (see Figure 5). Keep a position available for  $C_2$ , and be prepared to install a high-frequency capacitor of between 22pF and 150pF in case any jitter problem is noted.

### COMPENSATION WITHOUT LOAD-LINE REGULATION

The non load-line regulated converter is accurately modeled as a voltage-mode regulator with two poles at the L-C

resonant frequency and a zero at the ESR frequency. A type III controller, as shown in Figure 13, provides the necessary compensation.

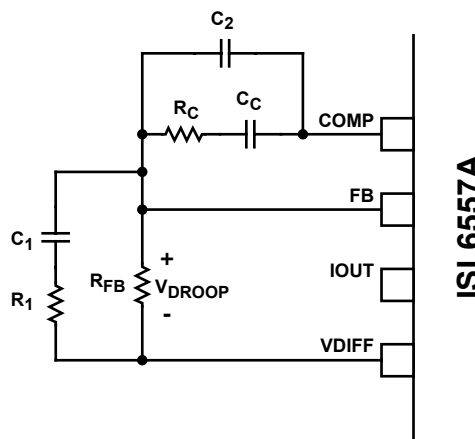


FIGURE 13. COMPENSATION CIRCUIT FOR ISL6557A BASED CONVERTER WITHOUT LOAD-LINE REGULATION.

The first step is to choose the desired bandwidth,  $f_0$ , of the compensated system. Choose a frequency high enough to assure adequate transient performance but not higher than 1/3 of the switching frequency. The type-III compensator has an extra high-frequency pole,  $f_{HF}$ . This pole can be used for added noise rejection or to assure adequate attenuation at the error-amplifier high-order pole and zero frequencies. A good general rule is to choose  $f_{HF} = 10 f_0$ , but it can be higher if desired. Choosing  $f_{HF}$  to be lower than  $10 f_0$  can cause problems with too much phase shift below the system bandwidth.

In the solutions to the compensation equations, there is a single degree of freedom. For the solutions presented in Equations 21,  $R_{FB}$  is selected arbitrarily. The remaining compensation components are then selected according to Equations 21.

$$R_1 = R_{FB} \frac{C(ESR)}{\sqrt{LC} - C(ESR)}$$

$$C_1 = \frac{\sqrt{LC} - C(ESR)}{R_{FB}}$$

$$C_2 = \frac{0.75 V_{IN}}{(2\pi)^2 f_0 f_{HF} \sqrt{LC} R_{FB} V_{PP}} \quad (EQ. 21)$$

$$R_C = \frac{R_{FB} V_{PP} (2\pi)^2 f_0 f_{HF} LC}{0.75 V_{IN} (2\pi f_{HF} \sqrt{LC} - 1)}$$

$$C_C = \frac{0.75 V_{IN} (2\pi f_{HF} \sqrt{LC} - 1)}{(2\pi)^2 V_{PP} R_{FB} f_0 f_{HF}}$$

In Equations 21, L is the per-channel filter inductance divided by the number of active channels; C is the sum total of all output capacitors; ESR is the equivalent-series resistance of the bulk output-filter capacitance; and  $V_{PP}$  is the peak-to-peak sawtooth signal amplitude as described in Figure 5 and “Electrical Specifications”.

### Output Filter Design

The output inductors and the output capacitor bank together form a low-pass filter responsible for smoothing the pulsating voltage at the phase nodes. The output filter also must provide the transient energy during the interval of time after the beginning of the transient until the regulator can fully respond. Because it has a low bandwidth compared to the switching frequency, the output filter necessarily limits the system transient response leaving the output capacitor bank to supply or sink load current while the current in the output inductors increases or decreases to meet the demand.

In high-speed converters, the output capacitor bank is usually the most costly (and often the largest) part of the circuit. Output filter design begins with minimizing the cost of this part of the circuit. The critical load parameters in choosing the output capacitors are the maximum size of the load step,  $\Delta I$ ; the load-current slew rate,  $di/dt$ ; and the maximum allowable output-voltage deviation under transient loading,  $\Delta V_{MAX}$ . Capacitors are characterized according to their capacitance, ESR, and ESL (equivalent series inductance).

At the beginning of the load transient, the output capacitors supply all of the transient current. The output voltage will initially deviate by an amount approximated by the voltage drop across the ESL. As the load current increases, the voltage drop across the ESR increases linearly until the load current reaches its final value. The capacitors selected must have sufficiently low ESL and ESR so that the total output-voltage deviation is less than the allowable maximum. Neglecting the contribution of inductor current and regulator response, the output voltage initially deviates by an amount

$$\Delta V \approx (ESL) \frac{di}{dt} + (ESR) \Delta I \quad (\text{EQ. 22})$$

The filter capacitor must have sufficiently low ESL and ESR so that  $\Delta V < \Delta V_{MAX}$ .

Most capacitor solutions rely on a mixture of high-frequency capacitors with relatively low capacitance in combination with bulk capacitors having high capacitance but limited high-frequency performance. Minimizing the ESL of the high-frequency capacitors allows them to support the output voltage as the current increases. Minimizing the ESR of the bulk capacitors allows them to supply the increased current with less output voltage deviation.

The ESR of the bulk capacitors also creates the majority of the output-voltage ripple. As the bulk capacitors sink and source the inductor ac ripple current (see *Interleaving* and Equation 2), a voltage develops across the bulk-capacitor ESR equal to  $I_{PP}(ESR)$ . Thus, once the output capacitors are selected, the maximum allowable ripple voltage,  $V_{PP(MAX)}$ , determines the a lower limit on the inductance.

$$L \geq (ESR) \frac{(V_{IN} - NV_{OUT}) V_{OUT}}{f_S V_{IN} V_{PP(MAX)}} \quad (\text{EQ. 23})$$

Since the capacitors are supplying a decreasing portion of the load current while the regulator recovers from the transient, the capacitor voltage becomes slightly depleted. The output inductors must be capable of assuming the entire load current before the output voltage decreases more than  $\Delta V_{MAX}$ . This places an upper limits on inductance.

$$L \leq \frac{2NCV_O}{(\Delta I)^2} [\Delta V_{MAX} - \Delta I(ESR)] \quad (\text{EQ. 24})$$

$$L \leq \frac{(1.25)NC}{(\Delta I)^2} [\Delta V_{MAX} - \Delta I(ESR)] (V_{IN} - V_O) \quad (\text{EQ. 25})$$

Equation 25 gives the upper limit on L for the cases when the trailing edge of the current transient causes a greater output-voltage deviation than the leading edge. Equation 24 addresses the leading edge. Normally, the trailing edge dictates the selection of L because duty cycles are usually less than 50%. Nevertheless, both inequalities should be evaluated, and L should be selected based on the lower of the two results. In each equation, L is the per-channel inductance, C is the total output capacitance, and N is the number of active channels.

### Switching Frequency

There are a number of variables to consider when choosing the switching frequency. There are considerable effects on the upper-MOSFET loss calculation and, to a lesser extent, the lower-MOSFET loss calculation. These effects are outlined in *MOSFETs*, and they establish the upper limit for the switching frequency. The lower limit is established by the requirement for fast transient response and small output-voltage ripple as outlined in *Output Filter Design*. Choose the lowest switching frequency that allows the regulator to meet the transient-response requirements.

Switching frequency is determined by the selection of the frequency-setting resistor,  $R_T$  (see the figure *Typical Application* on page 3). Figure 14 and Equation 26 are provided to assist in the selecting the correct value for  $R_T$ .

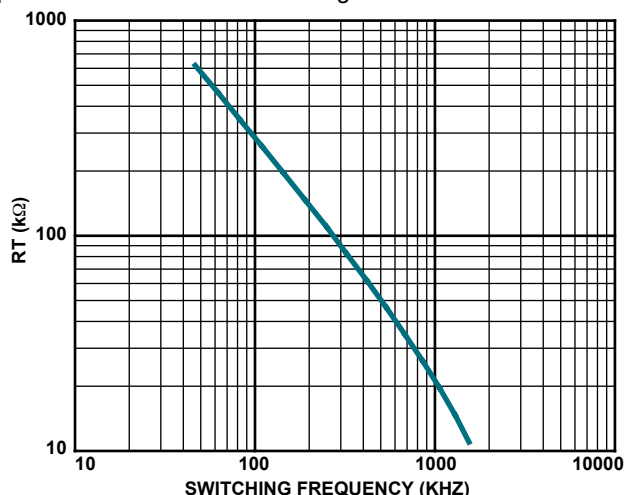


FIGURE 14.  $R_T$  VS SWITCHING FREQUENCY

$$R_T = 10^{[11.09 - 1.13 \log(f_s)]} \quad (\text{EQ. 26})$$

### Input Capacitor Selection

The input capacitors are responsible for sourcing the ac component of the input current flowing into the upper MOSFETs. Their rms current capacity must be sufficient to handle the ac component of the current drawn by the upper MOSFETs which is related to duty cycle and the number of active phases.

Figures 15, 16 and 17 can be used to determine the input-capacitor rms current as of duty cycle, maximum sustained output current ( $I_O$ ), and the ratio of the combined peak-to-peak inductor current ( $I_{L,PP}$  as defined in Equation 1) to the maximum sustained load current,  $I_O$ . Figure 18 is provided as a reference to demonstrate the dramatic reductions in input-capacitor rms current upon the implementation of the multiphase topology.

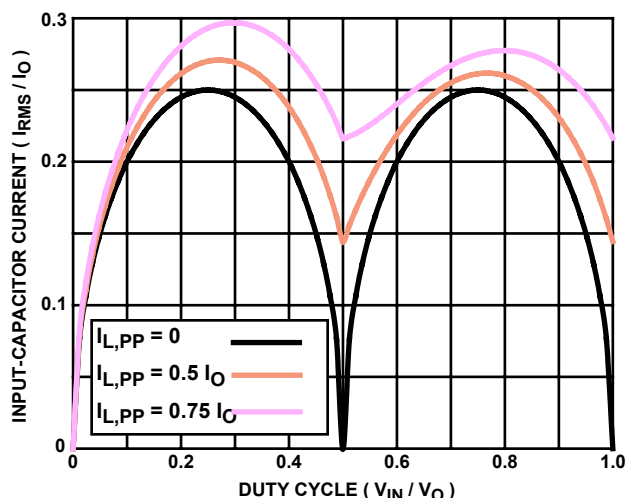


FIGURE 15. NORMALIZED INPUT-CAPACITOR RMS CURRENT VS DUTY CYCLE FOR 2-PHASE

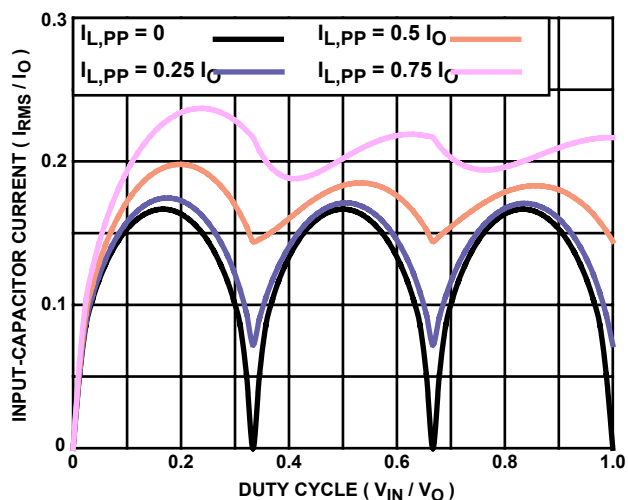


FIGURE 16. NORMALIZED INPUT-CAPACITOR RMS CURRENT VS DUTY CYCLE FOR 3-PHASE CONVERTER



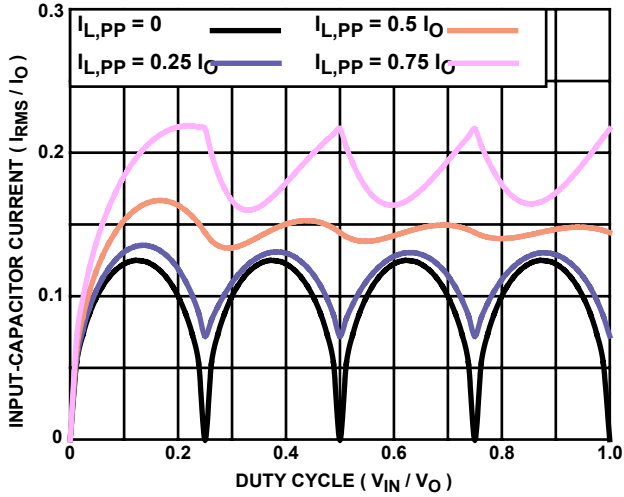


FIGURE 17. NORMALIZED INPUT-CAPACITOR RMS CURRENT VS DUTY CYCLE FOR 4-PHASE CONVERTER

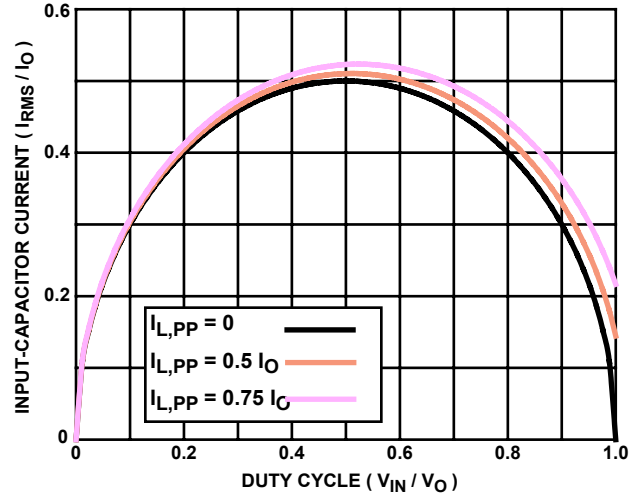
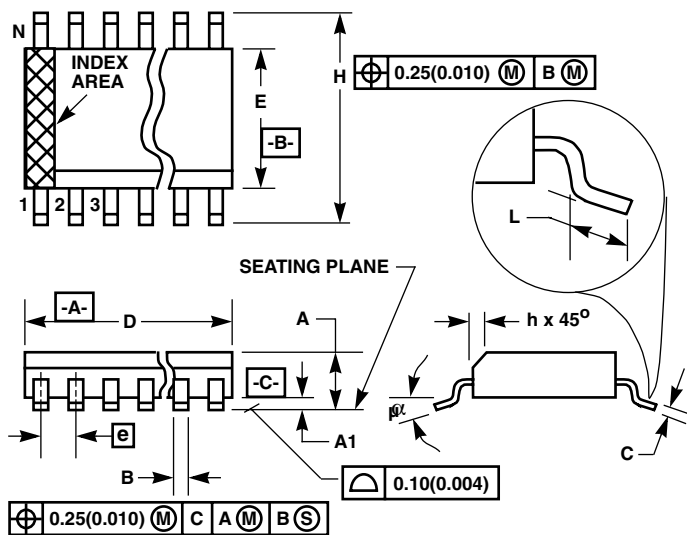


FIGURE 18. NORMALIZED INPUT-CAPACITOR RMS CURRENT VS DUTY CYCLE FOR SINGLE-PHASE CONVERTER

**Small Outline Plastic Packages (SOIC)**



**M24.3 (JEDEC MS-013-AD ISSUE C)  
24 LEAD WIDE BODY SMALL OUTLINE PLASTIC PACKAGE**

| SYMBOL   | INCHES   |        | MILLIMETERS |       | NOTES |
|----------|----------|--------|-------------|-------|-------|
|          | MIN      | MAX    | MIN         | MAX   |       |
| A        | 0.0926   | 0.1043 | 2.35        | 2.65  | -     |
| A1       | 0.0040   | 0.0118 | 0.10        | 0.30  | -     |
| B        | 0.013    | 0.020  | 0.33        | 0.51  | 9     |
| C        | 0.0091   | 0.0125 | 0.23        | 0.32  | -     |
| D        | 0.5985   | 0.6141 | 15.20       | 15.60 | 3     |
| E        | 0.2914   | 0.2992 | 7.40        | 7.60  | 4     |
| e        | 0.05 BSC |        | 1.27 BSC    |       | -     |
| H        | 0.394    | 0.419  | 10.00       | 10.65 | -     |
| h        | 0.010    | 0.029  | 0.25        | 0.75  | 5     |
| L        | 0.016    | 0.050  | 0.40        | 1.27  | 6     |
| N        | 24       |        | 24          |       | 7     |
| $\alpha$ | 0°       | 8°     | 0°          | 8°    | -     |

**NOTES:**

1. Symbols are defined in the "MO Series Symbol List" in Section 2.2 of Publication Number 95.
2. Dimensioning and tolerancing per ANSI Y14.5M-1982.
3. Dimension "D" does not include mold flash, protrusions or gate burrs. Mold flash, protrusion and gate burrs shall not exceed 0.15mm (0.006 inch) per side.
4. Dimension "E" does not include interlead flash or protrusions. Interlead flash and protrusions shall not exceed 0.25mm (0.010 inch) per side.
5. The chamfer on the body is optional. If it is not present, a visual index feature must be located within the crosshatched area.
6. "L" is the length of terminal for soldering to a substrate.
7. "N" is the number of terminal positions.
8. Terminal numbers are shown for reference only.
9. The lead width "B", as measured 0.36mm (0.014 inch) or greater above the seating plane, shall not exceed a maximum value of 0.61mm (0.024 inch)
10. Controlling dimension: MILLIMETER. Converted inch dimensions are not necessarily exact.

Rev. 0 12/93

All Intersil U.S. products are manufactured, assembled and tested utilizing ISO9000 quality systems. Intersil Corporation's quality certifications can be viewed at [www.intersil.com/design/quality](http://www.intersil.com/design/quality)

*Intersil products are sold by description only. Intersil Corporation reserves the right to make changes in circuit design, software and/or specifications at any time without notice. Accordingly, the reader is cautioned to verify that data sheets are current before placing orders. Information furnished by Intersil is believed to be accurate and reliable. However, no responsibility is assumed by Intersil or its subsidiaries for its use; nor for any infringements of patents or other rights of third parties which may result from its use. No license is granted by implication or otherwise under any patent or patent rights of Intersil or its subsidiaries.*

For information regarding Intersil Corporation and its products, see [www.intersil.com](http://www.intersil.com)

**Sales Office Headquarters**

**NORTH AMERICA**  
Intersil Corporation  
7585 Irvine Center Drive  
Suite 100  
Irvine, CA 92618  
TEL: (949) 341-7000  
FAX: (949) 341-7123

Intersil Corporation  
2401 Palm Bay Rd.  
Palm Bay, FL 32905  
TEL: (321) 724-7000  
FAX: (321) 724-7946

**EUROPE**  
Intersil Europe Sarl  
Ave. William Grasse, 3  
1006 Lausanne  
Switzerland  
TEL: +41 21 6140560  
FAX: +41 21 6140579

**ASIA**  
Intersil Corporation  
Unit 1804 18/F Guangdong Water Building  
83 Austin Road  
TST, Kowloon Hong Kong  
TEL: +852 2723 6339  
FAX: +852 2730 1433